TU Delft

Delft University of Technology

Document Version
Final published version

Citation (APA)
Peretz, E., Kurczynski, P., Johnson, M. D., Houston, J., Sridharan, T. K., Wang, J., Galison, P., Gamble, R., Gurvits, L., & More Authors (2024). The Black Hole Explorer: Astrophysics Mission Concept Engineering Study Report. In L. E. Coyle, S. Matsuura, & M. D. Perrin (Eds.), *Space Telescopes and Instrumentation 2024: Optical, Infrared, and Millimeter Wave* Article 130922F (Proceedings of SPIE - The International Society for Optical Engineering; Vol. 13092). SPIE. https://doi.org/10.1117/12.3019010

Important note
To cite this publication, please use the final published version (if applicable).
Please check the document version above.

Copyright
In case the licence states “Dutch Copyright Act (Article 25fa)”, this publication was made available Green Open Access via the TU Delft Institutional Repository pursuant to Dutch Copyright Act (Article 25fa, the Taverne amendment). This provision does not affect copyright ownership.
Unless copyright is transferred by contract or statute, it remains with the copyright holder.

Sharing and reuse
Other than for strictly personal use, it is not permitted to download, forward or distribute the text or part of it, without the consent of the author(s) and/or copyright holder(s), unless the work is under an open content license such as Creative Commons.

Takedown policy
Please contact us and provide details if you believe this document breaches copyrights.
We will remove access to the work immediately and investigate your claim.

This work is downloaded from Delft University of Technology.

The Black Hole Explorer: Astrophysics Mission Concept Engineering Study Report

Eliad Peretz[*1], Peter Kurczynski[1], Michael D. Johnson[2,3], Janice Houston[3], Tirupati Kumara Sridharan[4], Jade Wang[5], Peter Galison[6,7,2], Ronald Gamble[1,8], Daniel Marrone[9], Scott Noble[1], Gary Melnick[2], Leonid Petrov[1], Hannah Rana[2,3], Kari Haworth[3], Sheperd S. Doeleman[2,3], Sara Issaoun[3], Shahar Hadar[10,11], Alexandru Lupsasca[12], Edward Tong[3], Kazunori Akiyama[13,14,2], Ranjani Srinivasan[3], Dan Boroson[5], Guangning Yang[1], Tiffany Hoerbelt[1], Jeffrey Small[1], Mareki Honma[14,15], Bryan Bilyeu[5], Ed Canavan[1], Katia Shtyrkova[5], Robert Lafon[1], Lenny Paritsky[5], Laura C. Sinclair[16], Mark Silver[5], Leonid Gurvits[17,18], Yuri Kovalev[19], Robert Lehmensiek[4], Hua Jiao[1], Lindy Blackburn[2,3], Alexandra Brosius[1], Rick Butler[1], Andrew Chael[20,21], Dominic Chang[2,7], Koushik Chatterjee[2,3], Peter Cheimets[3], Daniel D'Orazio[22], Thomas Essinger-Hileman[1], Vincent Fish[13], Garret Fitzpatrick[3], Charles Gammie[23,24], Zachary Gelles[2,3,25], Michael Hecht[13], Jens Kauffmann[13], Jared Lucey[1], Chung-Pei Ma[26], Mark Matsumura[1], Daniel Palumbo[2,3], Dominic Pesce[3,2], Jeff Piepmeier[1], Christopher J. Roberts[1], Freek Roelofs[3,2,27], Paul Tiede[28,29], Jaye Verniero[1], Maciek Wielgus[19], Ed Wollack[1], George N. Wong[21,30], Kelsey Gilchrist[1], Kayla Carmical[1], Andrew Lewis[1], Maya Wertheim[1], and Keshet Shavit[1]

[1]NASA Goddard Space Flight Center, Greenbelt, MD 20771, USA
[2]Black Hole Initiative at Harvard University, 20 Garden Street, Cambridge, MA 02138, USA
[3]Center for Astrophysics, Harvard & Smithsonian, 60 Garden Street, Cambridge, MA 02138, USA
[4]National Radio Astronomical Observatories (NRAO)
[5]Massachusetts Institute of Technology Lincoln Laboratory, Lexington, MA 37235, USA
[6]Department of History of Science, Harvard University, Cambridge, MA 02138, USA
[7]Department of Physics, Harvard University, Cambridge, MA 02138, USA
[8]Department of Astronomy, University of Maryland-College Park, College Park, MD 20742, USA

Space Telescopes and Instrumentation 2024: Optical, Infrared, and Millimeter Wave, edited by Laura E. Coyle, Shuji Matsuura, Marshall D. Perrin, Proc. of SPIE Vol. 13092, 130922F · © 2024 SPIE · 0277-786X · doi: 10.1117/12.3019010

[9]The University of Arizona, Tucson, AZ 85721, USA
[10]Department of Mathematics and Physics, University of Haifa at Oranim, Kiryat Tivon 3600600, Israel
[11]Haifa Research Center for Theoretical Physics and Astrophysics, University of Haifa, Haifa 3498838, Israel
[12]Vanderbilt University, Nashville, TN 37235, USA
[13]Massachusetts Institute of Technology Haystack Observatory, 99 Millstone Road, Westford, MA 01886, USA
[14]National Astronomical Observatory of Japan, 2-21-1 Osawa, Mitaka, Tokyo 181-8588, Japan
[15]National Mizusawa VLBI Astronomical Observatory, Oshu, Iwate 023-0861, Japan
[16]National Institute of Standards and Technology, Boulder, CO 80303, USA
[17]Joint Institute for Very Long Baseline Interferometry European Research Infrastructure Consortium (JIVE), Oude Hoogeveensedijk 4, 7991 PD Dwingeloo, The Netherlands
[18]Delft University of Technology, Mekelweg 5, 2628 CD Delft, Netherlands
[19]Max-Planck-Institut für Radioastronomie, Auf dem Hügel 69, D-53121 Bonn, Germany
[20]Princeton Center for Theoretical Science, Jadwin Hall, Princeton University, Princeton, NJ 08544, USA
[21]Princeton Gravity Initiative, Princeton University, Princeton, NJ 08544, USA
[22]Niels Bohr Institute, University of Copenhagen, Copenhagen, Denmark
[23]Department of Astronomy, University of Illinois at Urbana-Champaign, 1002 West Green Street, Urbana, IL 61801, USA
[24]Department of Physics, University of Illinois, 1110 West Green Street, Urbana, IL 61801, USA
[25]Department of Physics, Princeton University, Jadwin Hall, Princeton University, Princeton, NJ 08544, USA
[26]Department of Astronomy, University of California - Berkeley, Berkeley, CA, USA
[27]Department of Astrophysics, Institute for Mathematics, Astrophysics and Particle Physics (IMAPP), Radboud University, P.O. Box 9010, 6500 GL Nijmegen, The Netherlands
[28]Department of Physics and Astronomy, University of Waterloo, 200

University Avenue West, Waterloo, ON, N2L 3G1, Canada
[29]Waterloo Centre for Astrophysics, University of Waterloo, Waterloo, ON, N2L 3G1, Canada
[30]Institute for Advanced Study, 1 Einstein Drive, Princeton, NJ 08540, USA

ABSTRACT

The Black Hole Explorer (BHEX) mission will enable the study of the fine photon ring structure, aiming to reveal the clear universal signatures of multiple photon orbits and true tests of general relativity, while also giving astronomers access to a much greater population of black hole shadows. Spacecraft orbits can sample interferometric Fourier spacings that are inaccessible from the ground, providing unparalleled angular resolution for the most detailed spatial studies of accretion and photon orbits and better time resolution. The BHEX mission concept provides space Very Long Baseline Interferometry (VLBI) at submillimeter wavelengths measurements to study black holes in coordination with the Event Horizon Telescope and other radio telescopes. This report presents the BHEX engineering goals, objectives and TRL analysis for a selection of the BHEX subsystems. This work aims to lay some of the groundwork for a near-term Explorers class mission proposal.

Keywords: The Black Hole Explorer, Black Hole, BHEX, Radio Emissions, Mission Concept, VLBI, Explorers Program, TRL

*Author for correspondence, Eliad.Peretz@nasa.gov

1. INTRODUCTION

The Black Hole Explorer (BHEX) is a space mission to image radio emissions of black holes by expanding both the baseline and time resolution of Very Long Baseline Interferometry (VLBI). This involves integrating a space telescope into an array of ground telescopes, such as the Event Horizon Telescope (EHT). Ultimately, the BHEX will enable transformative science, and its mission goals are well aligned with the Astro 2020 Decadal Survey.
The BHEX mission concept is a space-based component of a space-ground interferometer with a 3.5-meter antenna at medium Earth orbit (∼26,000 km orbital radius). The satellite will be equipped with a coherent dual-polarization dual-band receiver system covering 84-106 GHz and 240-320 GHz frequency ranges. The receiver system will allow simultaneous dual-band observations, leveraging frequency phase transfer techniques and phase stability at the lower frequency band to build sensitivity at the higher frequency band. The total downlink bandwidth from the satellite will be 64 Gbps.

The BHEX mission concept study was designed with three major stages: (1) a Science Study which articulates plausible goals and objectives (2) an Engineering Study which articulates overall feasibility and technological readiness and (3) a Mission Architecture Study which combines the results of the previous studies to match achievable science goals and objectives with feasible engineering to yield a plausible mission architecture.

In April 2022, the BHEX Science Study report was released and reviewed by an executive evaluation panel. The scientific goals and objectives of the BHEX mission were stated as follows: (1) Precision black hole measurements seeks to detect and study the photon ring around a supermassive black hole as a new window into the strong-field spacetime, (2) Black hole accretion and jets focuses on how black holes interact with accreting matter to produce jets of radiation, i.e. to learn how black holes shine, and (3) Black hole formation and demographics aims to study how supermassive black holes have affected the evolution of galaxies.

The BHEX Science Study report emphasized that NASA's Explorers program is the appropriate program to support a space VLBI mission within the next decade. Both a Small Explorer (SMEX) and a Medium-Class Explorer (MIDEX) mission are scientific investigations that can be developed generally in 40 months or less and executed on-orbit in 3 years or less. A SMEX proposal would be of smaller scope and a more focused science case, which could possibly be more suited for the BHEX mission.

This Engineering Study considers the overall feasibility and technological readiness of some of the major sub-systems considered to be utilized to achieve the BHEX science goals. This report complements engineering requirements that were formed as part of the Engineering workshop at the Goddard Space Flight Center(GSFC) in November 2023 (see Fig. 1).



Figure 1: The BHEX Engineering workshop at GSFC in November 2023.

2. TRL ASSESSMENT METHODOLOGY

In this section we adopted the Technology Readiness Assessment (TRA) methodology developed to accurately and unambiguously determine the Technology Readiness Level (TRL) over a wide variety of systems and subsystems.[1–6] TRA is a process that determines the need to develop technological advances into a system. The assessment process consists of determining the current Technology Readiness Levels (TRLs) and the difficulty associated with moving a system or subsystem from one TRL to the next, using an Advanced Degree of Difficulty Assessment (AD2).

The TRLs are assessed by following a set of seven evaluation criteria, including Functional Elements, System Definition, System Integration, Modeling and Simulation Tools, Performance

Validation, Environmental Validation, Operations and Sustainment. For each of these facets, a set of unambiguous questions are asked regarding each proposed technology to determine whether a technology has met a specific TRL level with respect to the BHEX mission requirements. The smallest TRL assessed across the seven facets will be the TRL of the overall system. Table 1 captures the TRL assessment methodology in detail.

	Facets / TRL	Functional Elements	System Definition	System Integration	Modeling and Simulation Tools	Performance Validation	Environmental Validation	Operations and Sustainment
Technology concept and/or application formulated.	2	Basic functional elements of technology have been identified.	An apparent engineering design approach has been identified.	System architecture defined in terms of basic functions to be performed.	Operational requirement of functional elements verified through modeling or simulation.	Preliminary performance predictions have been made for basic functional elements.	Critical functional experiments for operational environment are known.	N/A
Analytical and experimental critical function and/or characteristic proof-of-concept.	3	Operation of functional elements verified through modeling or bench-scale tests.	Definition of relevant operational environment defined for basic functional components.	A conceptual design of the integrated system has been defined.	Models exist to extent that computer analysis and simulations are possible.	Preliminary system performance measurements have been identified and estimated.	Modeling or experimental results show feasibility of basic functions in expected environments.	N/A
Component and/or breadboard validation in laboratory environment.	4	Subsystem tests in a simulated laboratory environment show element interfaces will function.	System performance metrics and test requirements have been defined for relevant operational environment. Life-limiting mechanisms identified.	Preliminary functional testing of integrated system completed at laboratory bench-scale.	Models developed to predict performance against system functional and performance requirements.	Functional testing of integrated (hardware and software) component or breadboard system.	Laboratory scale tests indicate components and subsystem interfaces will function in operational environments.	Operational needs for the intended application have been identified. Preliminary ConOps developed.
Component and/or brassboard validation in relevant environment.	5	Functional element and interfaces sufficiently understood at engineering scale to provide system design tradeoffs.	Prototypical system testing for the range of critical operational environments validates design. Characterize physics of life-limiting mechanisms and failure modes.	Integration challenges for engineering scale understood and resolved.	Models predict subsystem and integrated system performance in the operational environment.	Performance testing of integrated component or brassboard system.	System testing in approximate operational environment completed.	Component and/or brassboard demonstration of essential elements of the ConOps.
System/subsystem model for prototype demonstrated in a relevant environment	6	Functional elements and interfaces provide optimized system design.	Full-scale engineering design complete and documented.	Technology hardware and software demonstrated as an integrated system in a relevant environment.	Model subsystem and system predictions validated by engineering-scale testing and documented.	Performance of a high-fidelity engineering design unit demonstrated. Verify by test that the technology is resilient to the effects of life-limiting mechanisms.	Engineering-scale tests demonstrate functionality over full range of design critical environments.	System/subsystem demonstration of essential elements of the ConOps.
System prototype demonstration in an operational environment	7	System prototype functional elements and interfaces demonstrated for the intended operating environment.	High-fidelity system prototype developed using completed engineering design specifications.	Prototype fully integrated with intended system and demonstrated in operational environment.	Performance predictions verified by high-fidelity system prototype testing. Models validated with data from prototype operation.	Mission performance validated with data from prototype operations.	Design environments validated based on data from prototype operations.	Prototype demonstration of the ConOps. Preliminary demonstration of system operations and sustainment.
Actual system completed and "flight qualified" through test and demonstration.	8	Actual system functional elements and interfaces qualified for the intended operating environments.	Final engineering design and operational specifications are complete and verified.	Actual system qualified for an operational system in its intended environment.	Predicted performance for the final system design verified through tests. Models verified and validated per project M&S requirements.	Performance of the final system design validated with mission data. Life test unit for life limited items.	Design environments validated based on mission data. Completed life tests.	Compliance of actual system with design for operations and sustainment.
Actual system flight proven through successful mission operation.	9	System functions and interfaces of the actual system proven through successful mission operations.	Final engineering design and operation specifications are verified and validated.	Hardware and software fully integrated with operational system and demonstrated through mission operation. Sustaining software support is in place.	Predicted performance for the system verified through mission operations. Models verified and validated per project M&S requirements.	Performance predictions fully validated with data from mission operations.	Design environments and analyses validated based on data from mission operations.	Demonstration of system operations and sustainment.

Table 1: Technology Readiness Level Criteria Matrix

3. ENGINEERING SUBSYSTEMS

The engineering study provides an analysis of several BHEX subsystems, including the antenna in subsection 3.1, the cryocooler in subsection 3.2, frequency reference options in subsection 3.3, and optical communications in subsection 3.4. This study does not include the receiver, digital back end, optical data transmission, and the sampler and digital signal processor subsystems that will be discussed in later publications. After introducing the subsystem and its role in the BHEX mission, the engineering requirements are provided, allowing for a TRL assessment of possible subsystem solutions.

3.1 Antenna

3.1.1 Introduction

The antenna is the largest component of the BHEX science payload, capturing the mission's primary data. This section studies possible antenna solutions considering the design requirements such as aperture size and the frequency range derived from the science goals. Considering these parameters, current and future antenna systems are given a TRL assessment, using the methodology described in section 2 and suggesting a technology development path.

For more detail on the antenna subsystem, see "The Black Hole Explorer (BHEX): Preliminary Antenna Design".[7]

3.1.2 Engineering Requirements

The engineering requirements are derived from the mission's science goals that require operation frequencies up to 320 GHz. In order to achieve this, the spaceborne antenna must be highly efficient with a large aperture, high surface precision, and be as lightweight as possible without compromising performance: there is a target of a $\sim$3.5 m aperture, a mass of $\sim$50 kg, operation up to 320 GHz, and a surface rms less than 40 µm. The currently adopted baseline design is a Gregorian configuration, or axially displaced ellipse (ADE) optical design, and metallized carbon fiber sandwich realization to achieve a lower mass.

3.1.3 Technological Approaches

To fulfill these engineering requirements and choose an appropriate development path for the BHEX mission, we analyzed available antenna technology to determine the TRL of this subsystem. See table **??** for the parameters of current and target antenna solutions that were identified using industry capabilities, development timeline predictions, cost, and feasibility.

Monolithic One possible solution is a monolithic antenna formed from carbon fiber composites. Such an antenna was developed in conjunction with SBIR awarded to Vanguard Space Technologies[8] for the Balloon-Borne Large-aperture Submillimeter Telescope - The Next Generation (BLAST-TNG) (see fig. 3 and fig.2). This antenna has an aperture that measures 2.5 meters, which is on the smaller end of aperture sizes optimal for the mission. BLAST-TNG operated at a frequency range of 600 - 2000 GHz making the antenna's operable frequency range very suitable for the BHEX mission. Additionally, this antenna is part of a Cassegrain design

Model/ Mission	Vendor	Size m	Surface accuracy μm	Area density kg/m^{-2}	Efficiency[4] $\eta_{RuzeGHz}$ 86/230/320	Mass (3.5 m) kg	Bands	Technology
Herschel	Astrium-Airbus	3.5	< 10	25	1	210	THz/FIR	metallized SiC
Planck	Astrium-Airbus	1.6× 1.9	7.5-50	13	> 0.98[5]	125	mm - THz	metallized CFRP sandwich
BHEX (target)	-	3.5	< 40	~ 5	0.98/0.85/0.75	~ 50	mm/sub-mm	metallized CFRP sandwich
EarthCARE	NEC	2.5	< 60	-	0.95/-/-	-	mm	CFRP sandwich
Europa Clipper	AASC[1]	3	< 150	4	0.75/-/-	38	Ka	CFRP sandwich
FMR	L3 Harris	3.2	< 270	2.6	0.38/-/-	~ 25	upto V	mesh
PTR[2,3]	L3 Harris	2-22	< 250	2	-	~ 20	Ka	mesh
SDR[3]	Airbus	5	< 250	2.2	-	~ 20	X	CFRP

[1]Advanced Aerospace Structures Corp. [2]Perimeter Truss Reflector [3]deployed [4]estimates excluding reflectivity [5]based on predicted whole surface rms

Table 2: Space Antenna Technologies, see ref [7] for more detail

where the primary mirror is composed of carbon fiber and the secondary mirror is composed of aluminum, making it relatively lightweight. The secondary has tip/tilt and piston independent actuators. To consider the form factor, the secondary vertex is 1.59 meters from the primary;[9] the size is plausible for fitting in a reasonable rocket bearing. Ultimately, this antenna is an interesting development that is worth pursuing.

In the current marketplace, the Italian company Media Lario[10] has manufactured a 2.5 m antenna with 8 micron RMS surface for the ASTHROS balloon project at a cost of ∼750K. Media Lario uses a patented manufacturing method called Repli-formed Optics,[11] which they advertise as being similar to the method used to create antennas for the Atacama Large Millimeter-Submillimeter Array (ALMA).

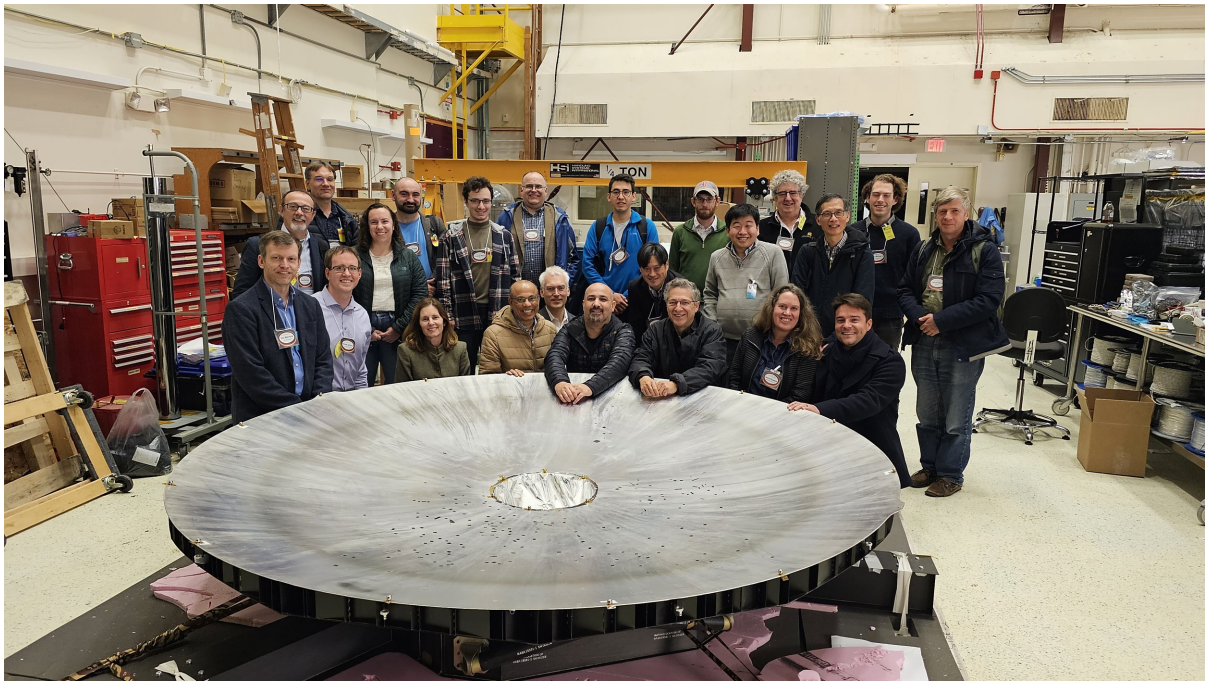

Figure 2: The BHEX team around surface tested BLAST-TNG antenna at Goddard Space Flight Center (GSFC).

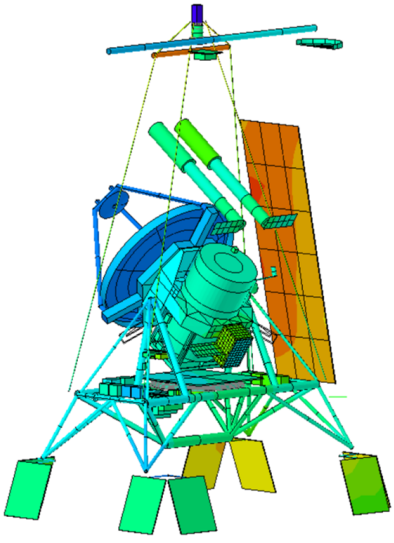

Figure 3: The Cassegrain imaging system, used in the BLAST-TNG experiment, with a 2.5 meter aperture antenna.[9]

Northrop Grumman mesh antennas Another possible solution is the Northrop Grumman AstroMesh unfurlable mesh antenna. This system can be produced with aperture sizes from 3 to 22 meters in diameter, providing a large range for various use cases. It is evident that the

AstroMesh antenna has proved its quality in previous missions: an AstroMesh system has flown in 10 different orbiting missions and all have performed as expected. It is simply the BHEX use case in which the Northrop Grumman mesh antenna's performance has not yet been proven as the system has only been proven to work at frequencies of $\leq$65 GHz.



Figure 4: A depiction of the Northrop Grumman AstroMesh antenna, positioned on the NASA Jet Propulsion Laboratory Soil Moisture Active/Passive mission, launched in 2015. Its technology was trusted by JPL in fulfilling a goal presented in the first Earth Science Decadal Survey.[12]

Airbus unfurlable antenna Another approach worth evaluation are the unfurlable antennas (see Fig. 5) manufactured by Airbus.[13] This design comes in aperture sizes of 2.5 through 5 meters, with a mass of 70 kg for 5 meters. One area that would require further engineering development and modification is the operating frequency. This design currently only operates up to $\sim$10 GHz. While Airbus has shown to understand the sources of error to improve surface quality, they do not have existing laboratory test fixtures or existing metalization facilities necessary to do the required work.

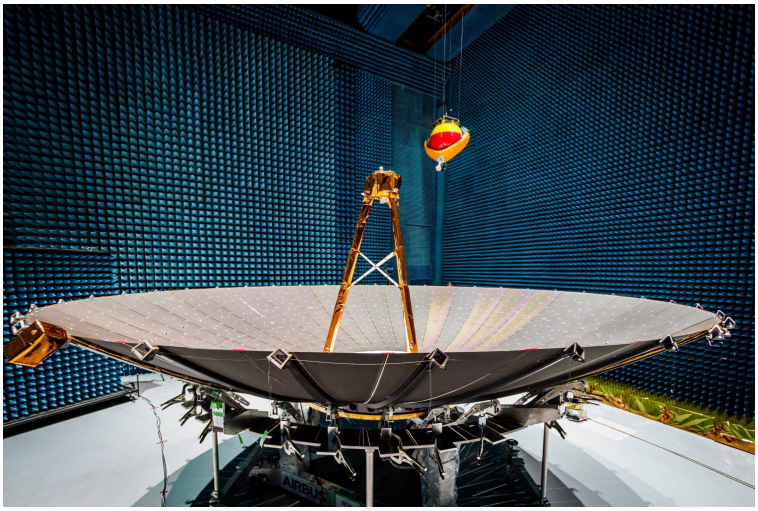

Figure 5: A 5 meter unfurlable antenna manufactured by Airbus.[13]

L.Garde inflatable antenna The inflatable antenna system is, at the current time and for the requirements of the BHEX mission, only a concept. Regardless, the system is being studied for potential use in OASIS, a MIDEX mission concept, and SALTUS, a Probe mission concept. Although the concept appears very promising, it is still in its very early development stages for a mission such as BHEX, only flown once (see Fig. 6). It requires extensive development before it can be properly considered for use in the BHEX mission.

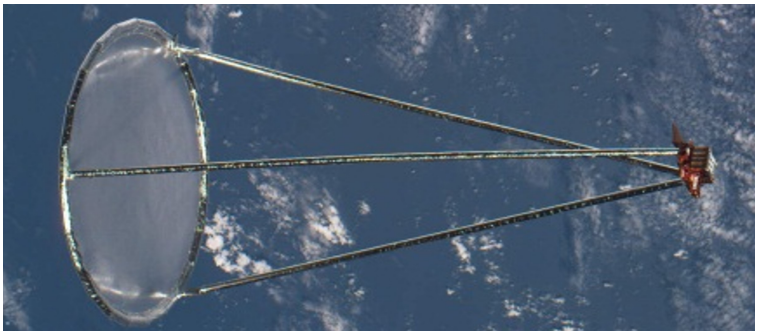

Figure 6: The L.Garde inflatable antenna experiment, flown on STS-77. The inflatable antenna includes a parabolic dish with a radius of 7 meters, attached to the body of the spacecraft using three 33 meter struts.[14]

MLS Another system assessed is the Microwave Limb Sounder (MLS) experiment that was incorporated in the NASA Aura spacecraft that was launched in 2004 (see Fig. 7). This system also has proven to operate in the necessary ranges of 100 - 300 GHz and was used with heterodyne radiometers in several frequency bands from ∼100 - 640 GHz. However, the diameter is only 1.6 meters. Additional information is necessary to determine if this system provides sufficient optical quality, but as long as the aperture size provides adequate sensitivity, this system is suitable for space VLBI.

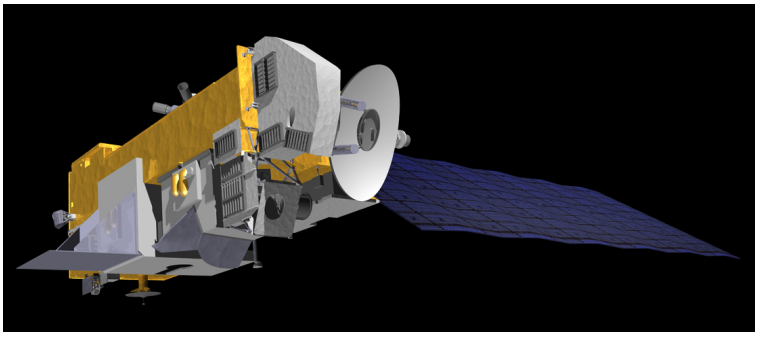

Figure 7: A depiction of the NASA Goddard Space Flight Center Aura spacecraft, equipped with MLS instruments. The spacecraft was able to use MLS to measure the temperature of Earth's stratosphere, as well as the content of Earth's upper troposphere.

3.1.4 TRL Assessments

Instrument	Technology Readiness Level (TRL)	Limiting Factor
BLAST-TNG	4-6	Has not launched in the environment of the BHEX mission
Northrop Grumman AstroMesh antenna	4-6	Not proven to work reliably in the required frequency range
Airbus unfurlable antenna	4-6	Has not been proven to operate in the BHEX mission environment or required frequency range
L.Garde inflatable antenna	3-4	Has not flown since a 1996 experiment; has been theorized to work for frequencies of up to only 60 GHz
MLS	4-6	Lacking sensitivity information

Table 3: Technology Readiness Level assessments for the components discussed in 3.1.3.

BLAST-TNG The antenna system used in the BLAST-TNG experiment has a TRL of 4-6 because the telescope was launched and operated at frequency levels in the range required by the BHEX mission. The limiting factors to this approach are that the BLAST-TNG experiment only operated in a sub-orbital launch and the small aperture size. In order to mature the TRL by 2025, it is necessary for the antenna to preform with a sensitivity sufficient for the mission's science objectives and in a relevant environment.

Northrop Grumman AstroMesh antenna The Northrop Grumman AstroMesh antenna has an assessed TRL of 4-6. It is being flown in various missions currently, including two Airbus Inmarsat-6 missions. While AstroMesh antennas have proven their reliability with a 100% success rate across more than 10 orbiting missions, it has not been proven to function properly with frequencies of 100 to 300 GHz, the required frequencies for the BHEX mission. While the AstroMesh antenna is completely developed in general, it requires further work to meet the BHEX mission requirements.

Airbus unfurlable antenna A TRL of 4-6 was assessed was the antenna manufactured by Airbus. A 5 meter unfurable antenna has been qualified for radar satellites and was scheduled to be launched in 2022. While being space-qualified, it is still necessary for the antenna be launched and preform in a relevant environment and needs further development as it currently operates in frequency ranges too low for the BHEX mission requirements.

L.Garde inflatable antenna The L.Garde inflatable antenna has been assessed to have a TRL of 3-4. Although it has flown in an experimental mission aboard STS-77, the 77th flight of the Space Shuttle, in 1996, it has not had additional flight experience. It has been conceptualized that the antenna will be able to function in Earth radiometry at frequencies ranging from 6 to 60 GHz,[15] well below the requirements for the BHEX mission. As it has only flown in an experimental mission, the L.Garde mission also has not proven itself to be qualified for to perform in the relevant enviroment and orbit ofr the BHEX mission.

MLS The MLS system has a TRL of 4-6 because it has been space-qualified and operated in the NASA Aura spacecraft in a sufficient frequency range. The spacecraft did not reach a HEO, so it would be necessary to test the antenna in an environment similar to the BHEX mission's. Additionally, it is unclear if the small aperture size of 1.6 meters would provide sensitivity levels adequate to reach the science goals. Maturing the TRL of this approach would entail further testing of the MLS and possible modification to increase its sensitivity.

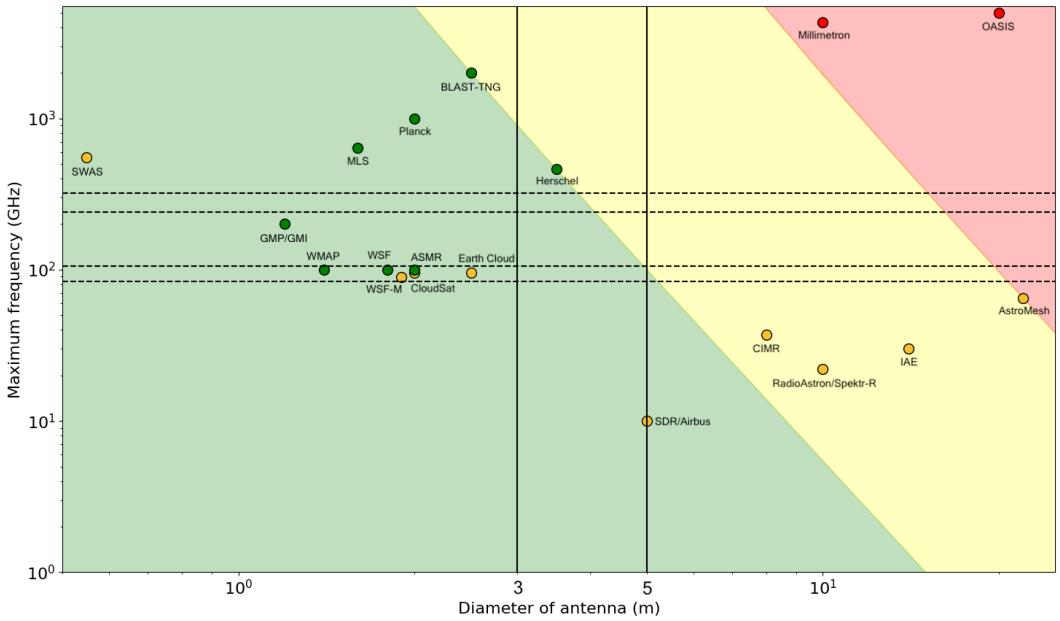

Figure 8: The diameters and maximum frequencies of the various systems described in this section. The color of the points represent the expected TRL in the year 2025. If the antenna is green, it is currently a TRL 6 or higher as it is in the advanced stages of development and meets the BHEX engineering requirements. The yellow points represent the antennas that could reach a TRL of 6 or higher by 2025, needing further development to meet the mission's requirements. Antennas with red points are unlikely to reach a TRL of at least 6 by 2025. The colored regions drawn using inferences made by the TRL of current technology illustrate the TRL of antennas with parameters in the designated region.[13,16–24]

3.2 Cryocooler

3.2.1 Introduction

In order for the cryogenics system to meet the science objectives and be suitable for an explorers class mission (SMEX/MIDEX), parameters such as mass and power will need to be balanced. This section discusses the engineering study done on the cryo cooler subsystem for the BHEX mission, including the engineering requirements and technology development path. For more details on the space heritage, trade space, and design of the BHEX cryocooler, see [25].

3.2.2 Engineering Requirements

The BHEX receiver suite necessitates cryogenic cooling to attain the desired receiver noise temperatures, approaching the quantum noise limit $T_{\mathrm{Q}} = h\nu/k$. The primary receiver's SIS mixers must be cooled to 4.5 K (about half the critical temperature of the SIS junction), while the secondary receiver's low noise amplifier needs to be cooled to 20 K. Notably, BHEX only requires a moderate heat lift to cool the receiver suite, without needing to cool the dish: the estimated heat load to be cooled is approximately 125 mW at 20 K and 10 mW at 4.5 K, with vibration tolerances around $5\,\mu$m.

3.2.3 Technological Approaches

Numerous design trade-offs are required to balance instrument operation and cryogenic system performance, ensuring both scientific objectives are met and the cryocooling system is suitably scaled for an explorers class mission (SMEX/MIDEX). For instance, the SIS mixers must operate at temperatures no greater than 4.5 K to achieve the necessary sensitivity for imaging the photon ring, dictating the power input and cooling power required from the cryocooler. Continuous operation of the cryocooler is essential to maintain receiver stability, as opposed to intermittent operation, which, while preventing power-saving measures, reduces contamination risk (the primary cause of cryocooler failure) and eliminates the need for cool-down and temperature stabilization for each observation cycle. Designing the BHEX cryogenic system involves balancing mass, power, and cost reduction within constraints while ensuring desired cooling performance, operation, and minimized failure risks.

There is an increasing demand for compact, efficient, closed-cycle cryocooling systems operating at 4 K for the next generation of space-based astronomy.[26] Past space missions featuring 4 K cooling stages include Planck[27] and Herschel;[28] more recent missions (e.g., SMILES/JEM, ASTRO-H, XRISM) incorporate closed-cycle 4 K cryocoolers using a combination of Stirling and Joule-Thomson (J-T) coolers. BHEX aims to utilize existing cryogenic technology, leveraging key components such as Stirling and J-T coolers, which have a proven spaceflight heritage.

Instrument	Temperature (K)	Cooling Power (mW)	Input Power (W)
Planck	4	-	-
JEM/SMILES	4.5	20	120
SPICA	1.7	10	180
BAE/Ball's	4	-	-
Key Laboratory of Space Energy Conversion Technologies	4.5	100	-

Table 4: Current Cryogenic Technologies for 4K-class Coolers

3.2.4 TRL Assessment and Technology Development Path

The cryogenic technological approach described above is assessed a TRL 4-6 at this time, while there are some commercial solutions with relevant specifications available, they are not tailored to the BHEX mission.

3.3 Frequency Reference

3.3.1 Introduction

In this chapter, we analyze solutions for the timing and coherence sub-system for BHEX. In particular, we focus on solutions for providing a sufficiently stable frequency reference to the BHEX instrument. The frequency reference serves two main purposes: to steer the synthesizer that generates the local oscillator frequencies in the receiver, and to provide a clock signal for the

digital back-end. Of these two purposes, the former sets the most stringent requirements, as the phase noise of the local oscillator at the highest observing frequency will determine the maximum coherent integration time. Here, the goal is to assess a wide range of possible technological approaches to determine those approaches which meet the engineering requirements with the lowest Size, Weight, and Power (SWaP) envelope and highest TRL.

3.3.2 Engineering Requirements

The main performance requirement is that the frequency reference shall introduce a coherence loss of less than 10% on a timescale of 10 seconds at an observing frequency of 345 GHz. This requirement assumes the use of the frequency-phase transfer technique and thus the critical metric arises from the fringe-searching timescale of the low-frequency band at 90 GHz. Losses introduced into the higher frequency band on this timescale will not easily be recovered unless the signal-to-noise ratio is very high in the high band. This is unlikely, particularly at the highest frequencies under consideration, so the requirement is set to ensure that no more than 10% signal loss is introduced by the space-based clock. An additional loss, that will also not be recovered, will be introduced by atmospheric turbulence during the fringe search period, and the clock should be sub-dominant. The choice of a timescale of 10 seconds is, in part, due to atmospheric turbulence-induced phase noise fluctuations which will significantly increase coherence loss under all but the best seeing conditions.

In evaluating frequency reference options, a connection has to be made between the presentation of reference performance in datasheets and scientific papers to the coherence requirement. Here, we first generate a model of the fractional frequency power spectral density (PSD) from the available frequency noise data. This PSD can then be integrated over with appropriate choice of filter functions leading to an estimate of coherence loss as a function of integration time. Figure 9 presents some of the resulting estimated maximum coherent integration times with a coherence loss of less than 10%.

To be compatible with the receiver and the digital back-end, the frequency reference shall output either a 10 MHz or 100 MHz signal. Note that this requires the use of an optical frequency comb laser to perform the necessary optical frequency division for any frequency reference that employs an optical carrier frequency. This signal will feed one or more frequency distribution systems which will ensure that the reference frequency is routed with sufficient signal strength to both the receiver and the digital back-end.

There is one additional requirement placed upon the frequency reference subsystem: the relation of the frequency reference to a time standard. Some of the technological approaches considered produce great stability over Fourier frequencies from 10 mHz to 5 kHz but do not provide long term accuracy. As a consequence, we also require that the BHEX frequency reference subsystem continuously measures the drift of the reference oscillator with respect to absolute time, with a precision of 1 ps/sec achieved when averaged over a period of 10 minutes. The frequency reference drift rate is essential to the data correlation. Continuous monitoring of it will ensure that the behavior of the frequency reference is well understood. To ensure that the drift rate is known with sufficient precision for correlation of any observation of a source, and to provide insurance against clock variability, a precise measurement should be available for every scan, for which 10 minutes is a representative duration.

3.3.3 Frequency Reference Options

There are a number of different approaches, both optical and microwave, to generating the required 10 or 100 MHz output with sufficiently low phase noise to support the performance requirement. A general rule of thumb is that approaches which divide down an optical oscillation to 10 MHz will outperform those which start from a microwave oscillation. However, often improved performance comes at the cost of system complexity, higher SWaP and lower TRL. These possible approaches can also be be divided into those that rely solely on a reference located on the BHEX platform and those that rely instead on frequency transfer from a ground station. Here, we present a range of different approaches.

Active Hydrogen Maser Upon first glance, active hydrogen masers are a particularly appealing option for the frequency reference for BHEX as they are the frequency reference currently in use by the EHT,[29] and thus are known to be able to support VLBI observations. Active hydrogen masers also have significant space heritage – two active hydrogen masers were flown for the Russian RadioAstron[30,31] mission. These masers had a mass of 60 kg and a volume of $\sim$480 L.[32] Additionally, the Space Hydrogen Maser (SHM) is being developed by the Nuchatel Observatory in Switzerland to be launched in the Atomic Clock Ensemble in Space (ACES)[33] mission aboard the International Space Station (ISS). However, the large SWaP envelope of active hydrogen masers along with their well known environmental sensitivity makes them a non-optimal choice of reference oscillator for the BHEX mission concept.

Ultra Stable Oscillators (USO) From a SWaP and a TRL perspective, use of an Ultra Stable Oscillator (USO) based on a temperature-controlled quartz crystal holds a great deal of promise. The challenge is finding a USO which can support the coherence requirement at the observing frequency of 345 GHz. One possible option is a USO developed by AccuBeat[34,35] currently serving in the European Space Agency's (ESA) Jupiter Icy Moons Explorer (JUICE) mission.[36] This out-of-family oscillator shows a phase noise performance that may meet the engineering requirements with the determination very sensitive to the exact choice of model parameters in connecting the datasheet of 34 to the simple modeling described in Section **??**.

Deep Space Atomic Clock A microwave clock based on a trapped mercury ion, named the Deep Space Atomic Clock (DSAC), was developed to support deep space navigation.[37] This 17 L, 44 W, and 17.5 kg clock has been shown to be robust and has been operated in space.[37] However, the fractional frequency instability given in Ref. 37 will not meet the coherence loss requirement, as our simple model predicts coherence loss of 90% at an averaging time of 0.6 seconds at 345 GHz.

Intermediate-Scale Optical Clocks An optical frequency reference can be formed by the stabilization of a continuous wave (CW) laser to an optical atomic or molecular transition. By referencing the output of an optical frequency comb to stabilized CW laser, the coherent optical pulse train output from the comb serves as the clock output and a microwave reference

frequency can be generated which preserves the fractional frequency instability of the CW laser. As atomic and molecular transitions can be quite narrow and probed with high signal-to-noise ratios, the resulting fractional frequency instability of the microwave output of the comb can be quite low. Here we will define intermediate-scale optical clocks to be those which achieve fractional frequency instabilities of $1 \times 10^{-13}/\sqrt{\tau} - 1 \times 10^{-14}/\sqrt{\tau}$, are centered on simple vapor cells, and do not require complex laser systems.

One possible type of intermediate scale atomic clock is based on a molecular iodine transition. Multiple iodine clocks have been operated continuously with performance that exceeds that of an active hydrogen maser over the timescales of interest even when located on-board a ship.[38] An iodine clock is also planned for the upcoming COMPASSO mission aboard the ISS.[39] In terms of SWaP, a commercial 30 L, 20 kg, 80 W instrument is currently available[35,40] with a technology development path that offers lower SWaP in the next one to two years.

Another intermediate-scale optical clock can be based on a 2-photon transition in rubidium. Commercial 2-photon rubidium clocks are now available with a similar 30 L and < 30 kg form factor.[35,41] These clocks have a similar technology development path to lower SWaP in the next one to two years.

State-of-the-Art Optical Clocks State-of-the-art optical clocks, unlike intermediate-scale optical clocks, probe even narrower atomic transitions and operate with the atoms confined in a trap to minimize broadening of the transition and systematics.[42] These are exquisite frequency references which can be compared at 18 digits;[43] however, these are not low SWaP instruments and development of transportable versions remains a research project.

Optical Frequency Division of a Cavity-Stabilized Laser As the frequency reference must provide low enough relative phase noise over Fourier frequencies from 10 mHz to 5 kHz, it is intriguing to consider a laser stabilized not to an atomic or molecular transition, but rather an optical artifact (optical cavity). This is particularly true in light of the use of a cavity-stabilized laser on-board the GRACE-FO mission[44] and the development of a cavity-stabilized laser for the LISA mission.[45] Unlike both GRACE-FO and LISA, which use the stable CW laser directly for optical interferometry, here, the stable CW laser frequency must be divided down to the microwave through use of an optical frequency comb. This need for optical frequency division (OFD) reduces the system technology readiness level (TRL) as well as increases the total SWaP due to the presence of the comb. As both optical clocks and OFD using a cavity-stabilized laser rely on the same core frequency comb technology, an improvement in this technology for one frequency reference will directly impact the other.

Another challenge in assessing the use of optical frequency division of a cavity-stabilized laser is determining which cavity-stabilized laser to employ. The larger cavity-stabilized lasers of Refs. 44 and 45 will meet the performance requirements for BHEX but will lead to an undesirable total system SWaP. Recent research has shown that miniaturization of optical cavities is possible;[46] however, this reduces the current TRL and critically reduces performance. A frequency reference which follows the data of Ref. 46 will not meet the performance requirements of BHEX. With

additional technology development, it is likely that a middle ground between the cavity-stabilized lasers of Refs. 44 and 46 combined with advancements in optical frequency combs could lead to a reference which meets the requirements of BHEX in a reasonable SWaP envelope.

Optical Time Transfer Two-way optical time transfer (O-TWTFT) based on either the RF modulation of the optical carrier associated with the optical communications system[47] or based on the transmission of optical frequency comb pulses[48,49] could meet the performance requirement. Frequency comb-based optical time transfer has been demonstrated over 300 km terrestrial distances with an ability to sustain link losses of greater than 100 dB. Although this is appealing, the SWaP-envelope for a timing node is on the order of 20 L, 15 kg and 50 W, excluding the free-space optical terminal. The TRL level for the SWaP-envelope is the same as the optical-communications based time transfer at a level 3. With a shift away from a geosynchronous orbit, more technological developments are required for both of these approaches to be able to handle the significant Doppler shifts occurring with relative motion of km/sec. Additionally, any two-way optical time transfer approach will require the optical link to be available during the observation period to maintain the frequency reference performance – this places a strict timeframe requirement upon the optical communications ground stations.

Microwave-based Time Transfer A two-way microwave time transfer that uses the a two-way carrier phase (TWCP) approach of Ref. 50 should be able to support the requirements of BHEX. This is a more advanced approach to microwave-based time transfer than the more conventional two-way satellite time-frequency transfer (TWSTFT) which would not meet the engineering requirements. However, for a system which plans to rely on an optical communications data downlink, use of this TWCP would signficantly increase the SWaP envelope of the overall BHEX mission; this method would require a dedicated high-power microwave transmitter and receiver.

Comparison of References Here, we have chosen to focus on frequency references located on the BHEX platform rather than methods of time/frequency transfer. Use of time/frequency transfer to steer an on-board oscillator could in some cases reduce the on-board oscillator complexity; however, it comes at the cost of additional receivers and the need for visibility for the time/frequency transfer system during the observing time. The latter cost arises because any on-board oscillator that provides sufficient holdover to not require active steering during the observation period is sufficient to not require the time transfer to begin with.

Figure 9 provides an estimate through integration over filtered versions of the modeled PSDs of Figure **??** of the maximum integration time for which the coherence is greater than 90% for a carrier frequency of 345 GHz. (See also Appendix **??**.) Note that this estimate does not take into account the limitation imposed by atmospheric turbulence or by the performance of the frequency reference at the ground site. From this simple model, it is clear that an active Hydrogen maser, an intermediate-scale optical clock based either on a molecular iodine or 2-photon rubidium transition, or optical frequency division from a cavity-stabilized laser will meet the engineering requirement. The case of the ultra stable oscillator is very interesting because it

sits right on the edge of the performance metric; thus, small errors in assumptions or modeling could provide an incorrect assessment of whether this frequency reference meets the performance metric.

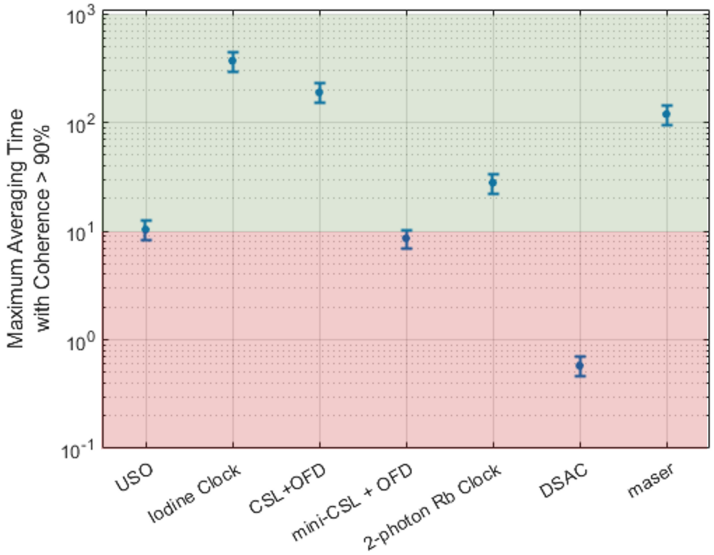

Figure 9: Model of maximum possible integration time with coherence greater than 90% for a 345 GHz carrier. This is looking at the contribution only from the frequency reference itself and does not include the limit of the atmosphere or the frequency reference at the other end of the baseline. Crude error bars were generated assuming a 20% error in the modeled PSD. The ultrastable oscillator (USO) datapoint was based on data from 34, the iodine clock from 38, the optical frequency division with a cavity-stabilized laser (CSL + OFD) from 44, the 2-photon rubidum clock (2-photon Rb clock) from 41, the optical frequency division from a miniaturized cavity-stabilized laser from 46, and the deep space atomic clock from 37. A a datapoint from modeling the active hydrogen maser (maser) from the first EHT results is also provided for reference.[29]

3.3.4 TRL Assessments

It is not only performance with which the frequency references must be assessed for BHEX but also their readiness compared to the proposed timescale and SWaP envelope of each. The choices of reference oscillator span a wide range of technology readiness levels (TRLs) as can be seen in Table 5.

Instrument	Technology Readiness Level (TRL)	Limiting Factor
Active Hydrogen Maser	4-5	Large volume / unreliable
USO	6-8	Phase noise may not meet requirement
Intermediate-Scale Optical Clock	3-5	Increasing TRL and SWaP reduction
Cavity-stabilized laser OFD	3-4	High phase noise for low-SWaP versions; high SWaP for sufficient performance versions

Table 5: Current Technology Readiness Level assessments for a selection of the components discussed in Section 3.3.3 most likely to meet BHEX requirements. The choice of TRL 6 for the active hydrogen maser (AHM) reflects the reliability issues of the RadioAstron masers[31] and the on-going development efforts for the ACES mission.[33] The choice of TRL 6-8 for the USO assumes that its phase noise does in fact meet the requirement. AHM: Active Hydrogen Maser; USO: ultra stable oscillator; OFD: optical frequency division

3.3.5 Technology Development Path

The simple modeling presented here for the ultra stable oscillator leads to uncertainty as to whether this reference choice meets the performance requirement or not. Characterization of the fractional frequency noise PSD of the ultra stable oscillator against a high quality laboratory reference or use for terrestrial VLBI observing at 345 GHz would clearly answer if it met the performance requirements. Alternatively, modifications to the ultra stable oscillator design that resulted in a reduction of the fractional frequency noise PSD would result in a reference that met the performance requirements.

For the intermediate-scale optical clocks, performance of existing ∼30 L units is not an issue. Rather the challenge lies in further SWaP reduction and space qualification. On-going technology development campaigns[51,52] forecast the development of intermediate-scale optical clocks with similar levels of performance but with form factors of ∼5 L, ∼10 kg, and ∼40 W within the next few years compatible with the BHEX timeline.

The technology development path for optical frequency division (OFD) of a cavity-stabilized laser (CSL) involves the investigation of a series of trades to arrive at a low-enough-SWaP system that meets the performance requirements. Because of this, even though some cavity-stabilized lasers themselves sit at TRL 9,[44] significant efforts are required both for the optical frequency comb development necessary for optical frequency division of the carrier and for reducing cavity size in order to match the projected SWaP of future intermediate scale optical clocks.

Our current recommendation is the use of an intermediate-scale optical clock as the frequency reference with an ultra stable oscillator serving as a backup. This is driven by the current low TRL combined with the performance of intermediate-scale optical clocks versus the high TRL

with uncertain sufficiency in performance of the ultra stable oscillator. In the case of failure of the intermediate-scale optical clock, some science goals could assuredly be met with the ultra stable oscillator. If additional testing and modeling suggests that the ultra stable oscillator meets the performance requirement, then frequency reference could be de-scoped to just the ultra stable oscillator, SWaP requirements for the timing and coherence subsystem. Likewise, given the rapid pace of maturation of intermediate-scale optical clocks, it may be possible at a later point to again de-scope and just use the intermediate-scale optical clock.

3.4 Optical Communications

3.4.1 Introduction

Optical (free-space laser) communication enables high-efficiency data transfer over large distances because it presents fewer diffraction losses along with greater bandwidth and power flexibility as compared to traditional radio frequency (RF) communications. BHEX revolves around precision measurement as the future of black hole science, but poses a challenge of data transfer. Precision measurement generates massive amounts of data that must be delivered from orbits capable of carrying out the same precision measurements given restraints on terminal size and power. Optical communication technology promises a solution.[53]

This analysis of optical communication primarily revolves around achievable downlink data rates – the amount of data that can be transmitted from the space terminal to the ground architecture per unit time. Scalability of the downlink rate to preserve resources is also discussed as an engineering requirement, along with the uplink data rate. Additionally, buffer size and buffer data access rates are taken into account especially considering latency, the delay before complete transfer of data. Finally, we consider the availability, the probability that data can be accessed, in relation to flight dynamics and ground system architecture. Bit error rate, the percent of errors relative to the total transmission, is only briefly addressed due to the time constraints of the study.

This study gives approximate data rates, and it is likely that real downlink data rates will fall below our achievable estimates in average conditions. Downlink data rate is dependent on the ground architecture, the space terminal design, and environmental factors. In this study we focus on how data rate is impacted by the range, the distance between the ground architecture and space terminal; the aperture size of the transmitter on the space terminal; the power of the amplifier on the transmitter; and the size of the ground telescope. We briefly touch on the alignment of the space terminal with the ground telescope as well.

The following missions' downlink technologies represent the current state of the art: LLCD (Lunar Laser Communication Demonstration, 2013), LCRD (Laser Communications Relay Demonstration, 2021), TBIRD (TeraByte Infrared Delivery, 2022), Psyche (2023), and Artemis II O2O (2025). Based on their achieved (or predicted) downlink data rates with varied mission parameters, we identify what downlink capabilities are currently possible and what is going to be possible in the near future. By projecting these missions' data rate performances onto BHEX requirements, we can analyze the timeline, cost, and feasibility of building a communication system that meets BHEX engineering requirements.

3.4.2 Engineering Requirements

Link Data Rate Downlink data rate is impacted by four main factors: the size of the space terminal transmission aperture, the power to the space terminal transmission amplifier, the size of the ground telescope, and the link range. Due to baseline sensitivity requirements of photon ring measurements, BHEX should be able to achieve a downlink data rate of greater than 64 Gbps from its orbit.

Link range, the distance between the space terminal and the ground architecture, has one of the largest impacts of the four main factors. Data rate scales inversely to the square of the range, which means that slight increases in range have large negative impacts on the flux at the ground station. Therefore, the medium Earth orbit intended for BHEX would be more resource-intensive than a system designed for LEO, and we will consider this most resource-intensive concept as the basis for analysis.

The design of the space terminal—mainly the size of the transmission aperture and the power to the transmission amplifier—also impacts the data rate. As signal exits the terminal at a given flux density, the total flux scales with the area of the aperture. Since aperture size is measured in diameter, the data rate scales directly with the square of the aperture size. Additionally, the power directed to the signal amplifier in the space terminal transmitter scales directly with the data rate. Finally, we must account for differences in ground telescope area, which scales directly with data rate. Telescope size is expressed in diameter, so data rate scales directly with the square of the telescope size.

Taking into account these major design factors—power, aperture size, range, and ground telescope size—we can develop an approximation equation for scaling where R_0, r_0, a_0, P_0, and d_0 are the starting data rate, range, aperture size, amp power, and telescope size, respectively:

$$R_{data} = R_0 \frac{r_0^2}{r^2} \frac{a^2}{a_0^2} \frac{P}{P_0} \frac{d^2}{d_0^2} \tag{1}$$

By using this equation and data rate estimations from existing technology, we can calculate which combinations of design parameters will result in a downlink rate of greater than 64 Gbps. Crucially, we can also identify which parameters are scalable during the mission to optimize resource use, since the transmitter will have varying data rate needs. Original link budget calculations from various missions are calculated accounting for efficiency, atmospheric losses, miscellaneous losses, and sensitivity, all of which are approximated to constants but can vary with wide deviation from original measurements.

We must also contend with the fact that the signal will attenuate through the atmosphere based on the alignment of the ground station and the space terminal, suggesting that some overhead should be allotted in terms of the maximum achievable downlink data rate or the availability of the ground stations. However, this is not examined more in depth in this study beyond Figure 10.

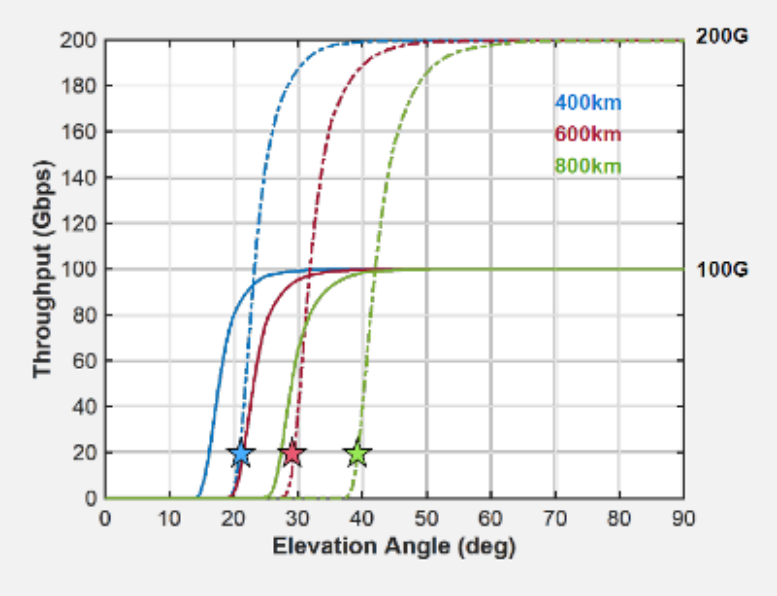

Figure 10: Throughput of TBIRD by elevation angle. Predicted TBIRD signal from LEO to a 40 cm diameter ground terminal using a 0.5 W transmitter and 1 cm transmission aperture.

The required uplink data rate is relatively small compared to the downlink data rate, as BHEX only requires around 3 kbps. This uplink rate is driven primarily by an Automatic Repeat Request (ARQ) system, which reduces bit error rate but requires the ground station to send data back to the space terminal to verify the coherence of data transmission.

Latency and Bit Error Rate Latency and bit error rate are intertwined, as both are directly related to the buffer system. Due to the large quantity of precision data that needs to be communicated, we desire a latency of "semi-real-time" and minimal data loss, which can be achieved using an ARQ method, which provides redundancy of data transmission for natural data loss. As a result, data needs to be stored as it is transmitted with a data access rate that is at least the downlink data rate. Not including overhead, onboard buffer storage should reach at least 10 GB while the data access rate of the drive should reach at least 64 Gbps. However, ARQ increases the latency, and a balance between the two can be achieved with sufficient downlink and uplink data rates.

Availability Availability is dependent primarily on ground system architecture – how many sites are used, where the sites are, and what percentage of the time will there be a cloud free line of sight (CFLOS) to the space terminal. Optical communication can achieve high data rates compared to its radio frequency (RF) counterparts, but it is particularly sensitive to cloud cover.

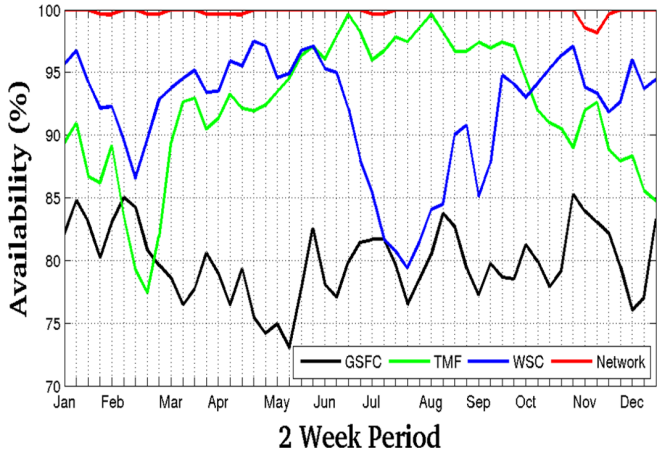

Figure 11: Probability of availability by ground system. Figure provided by Northrop Grumman, showing the probability of availability for an approximately 1 hour duration link from Artemis II to ground stations located at White Sands Complex in New Mexico, JPL's Table Mountain Facility in southern California, and Goddard Space Flight Center. The probabilities calculated assume that O2O has flexibility to schedule when it will establish a link during the day; essentially it is the probability that a station will have CFLOS to the spacecraft sometime during the day for ∼1 continuous uninterrupted hour.

112° West	
Sites	Mean Availability
Haleakala	69.6
TMF	65.7
White Sands	58.7
Livermore	60.4
Haleakala, TMF	89.0
Haleakala, TMF, WSC	94.7
Haleakala, TMF, WSC, Livermore	**97.3**
Haleakala, TMF, WSC, Livermore, GSFC	**98.4**
Haleakala, TMF, WSC, Livermore, GSFC, Kennedy	**99.1**
Haleakala, TMF, WSC, Livermore, GSFC, Kennedy, McDonald Observatory	**99.4**

Table 6: Example site lineup assuming LCRD located at 112-degrees West, 20-degree minimum elevation angle. Provided by Northrop Grumman, optimized over 1995-2015.

As seen in Fig 11, no one site will have 100 percent availability, but a combined 100 percent availability is approachable by placing multiple ground stations at multiple locations. BHEX scheduling needs will likely be very different, however the methodology remains the same. The locations selected will need to have uncorrelated weather. Availability will be largely dependent on location, but with two sites an 85 percent availability should be achievable. Four sites should provide sufficient availability for BHEX to operate optimally, as demonstrated in Table 6.

In addition to the ground system architecture, availability is impacted by flight dynamics since the elevation angle must be large enough to achieve throughput as seen in Figure 10. The

orbit of the space terminal will determine how often the space terminal is at acceptable elevation angles, and therefore determine how many ground telescopes are needed for adequate cover.

3.4.3 TRL Assessment

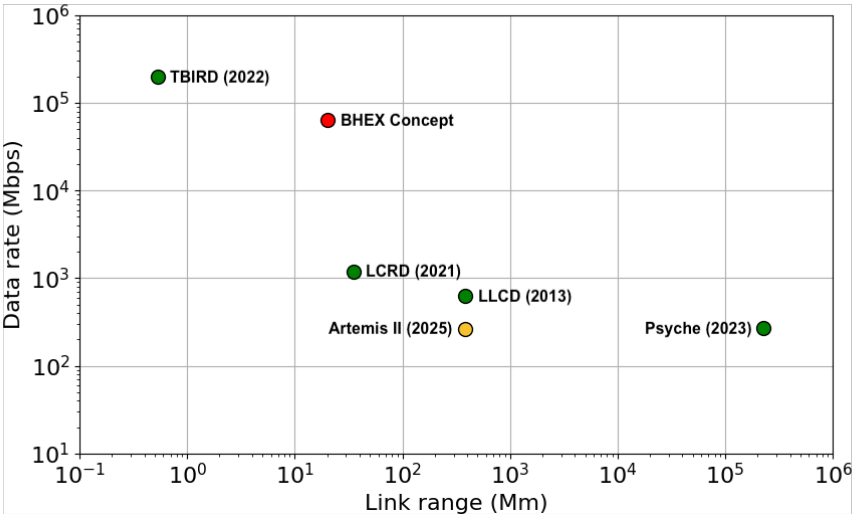

Figure 12: Mission downlink capabilities given by data rate versus link range, color coded by TRL. Green represents a mission that will be at least TRL 6 in the next year, while yellow represents TRL $\geq$ 6 in the next three years. BHEX Mission Concept is shown in red, not expected to reach a TRL $\geq$ 6 in the next three years.[23,24]

Space Terminal Of the high speed buffer, the high speed interfaces, the modem with ARQ, the high-power amplifier, and the optical module, the high-power amplifier and high speed buffer are the main drivers. The TBIRD Modem with ARQ, which can be used for BHEX with slight modifications, is TRL 9. The high-speed interfaces are also TRL 9. The 10 cm optical module, which needs to be modified to accommodate a high-power amplifier, is TRL 9. With the modifications, all technologies can be determined to hold a TRL level of 3-6, due to the necessity of modification of power, range, and other factors.

There are a variety of high-power amplifier options that present a variety of specifications at different TRL levels.

Currently, there do not seem to be any buffers that support required data writing speeds, thus the buffer is TRL 3, but this is a continued conversation with vendors.

Ground System The ground terminal consists of an optical telescope, modem with ARQ, and a high speed ground interface to a data sink. All ground terminal aspects are TRL 6-8.

3.4.4 Technology Development Path

For the BHEX optical communication system, the space terminal should include a high speed buffer with high speed interfaces to the EHT sensor as well as to the communications module. The communications module consists of a modem with ARQ, a high-power amplifier, and an optical module (telescope). This technical assessment will go in-depth into the TBIRD Modem and high-power amplifiers. The current BHEX concept for the space terminal requires a 10 cm optical telescope aperture working in conjunction with a 70 cm ground telescope and adaptive optics.

The ground terminal consists of an optical telescope, modem with ARQ, and a high speed ground interface to a data sink.

TBIRD Modem Case Study Using Eqn. 1, we can project an estimated data rate (R_{data}) for BHEX if it were to use any given mission's technology with our desired mission parameters: r, a, P, and d. TBIRD is the closest potential technology that would meet the mission requirements, so we calculate the projected data rate below for BHEX parameters.

TBIRD is capable of 200 Gbps from LEO to a 40 cm ground terminal using a 0.5 W transmitter with a 1 cm aperture.[54] Moving TBIRD from LEO to GEO will decrease the signal strength at the ground terminal approximately 10,000x. Increasing the aperture and telescope sizes to 10 cm and 70 cm, respectively, will increase the signal strength by factors of 100 and 3, respectively. Overall, this results in an overall factor of 0.12x, which results in a data rate of 12 Gbps. This means simply adopting TBIRD technology with the proposed BHEX transmitter and ground architecture parameters would not meet engineering requirements.

However, by scaling the power up or by further increasing transmitter aperture size and the size of the ground telescope, sufficient data rates can be achieved. Increasing the telescope size, increasing the power to the amplifier in the transmitter increases the data rate. As an example, with a 0.7 m telescope size, 128 Gbps could be achieved with 10.7 W, not accounting for overhead. Given this, a modified TBIRD modem would meet engineering requirements of $>$ 64 Gbps.

High-Power Amplifiers Power is extremely scalable and amplifier power can be optimized for efficiency and resource conservation based on how much data needs to be transmitted at a time.

Currently, commercially available space-qualified amplifiers are only suited for up to 5 W of applied power. As a result, 10 cm optical modules (the largest space-qualified optical telescopes) have only been demonstrated up to 5 W. However, 10-15 W amplifiers are in development or considered "low risk" by multiple vendors, which would allow for combinations of amplifiers to achieve power goals in lieu of increasing ground telescope size. However, combinations of these amplifiers would also require high-power wavelength division muiltiplexing (WDM).

For uplink technology, ground-based amplifiers supplied by PPM have been used for up to 50 W, which means they could easily be populated for 12 W loads. Using two would provide redundancy and significant lifetime since they are built for 24/7 use over a 5-10 year period.

Ground Telescopes Leveraging a network of large telescope facilities as downlink receivers could provide adequate availability coverage while increasing the data rate of a TBIRD-inspired space terminal. In addition to Keck, other telescope options include the Discovery Channel 4 m telescope at Lowell or the University of Hawaii's 2.2 m telescope on Mauna Kea. With these large telescopes, however, the tradeoff between power and telescope size relative to data rate in Eqn. 1 falls apart since there is a power "floor" created by adaptive optics requirements. Therefore, there are decreasing returns on increased telescope sizes. Additionally, these telescopes are not optimized for optical communication, which creates a larger operating cost.

In addition to the large telescope network discussed above, a 70 cm Low Cost Optical Terminal (LCOT) is currently in development at GSFC as a flexible optical terminal that is able to support optical from LEO to Lunar ranges. The concept is to build a single design that can support all optical communication missions from LEO to lunar distances, starting with a 70 cm diameter telescope, and making it modular and reconfigurable so that one system can be quickly reconfigured to support different missions, with the goal of organically growing a network of LCOTs as they are needed. The vendor that supplied the telescope is interested in the possibility of making 1-2 meter versions of the telescope. It has a COTS Adaptive Optics system that is currently being tested at GSFC. This is extremely relevant to BHEX given that going from a 70 cm telescope to a 1m telescope reduces the power requirement by a factor of 2, and using a telescope optimized for optical communication allows for lower error rates and reduced power usage when in operation.

The total cost of the ground terminal network also depends on how many telescopes are needed to achieve required availability.

Buffer The ARQ buffer needed for streaming downlink from GEO is different from LEO requirements in that it always has a line-of-sight. In optimal conditions when the link is operating, the buffer capacity does not need to be more than around 10 Gbps.

Previous discussions (2 years ago) between MIT-LL and vendors (SEAKR and 3Dplus) indicate there are space-qualified solutions in the 10's of Gbps range have flown. Further discussions with commercial vendors suggest that the driver is the access rate, not the buffer size. Likely, any buffer with 128 Gbps access rates will have storage on the order of 0.5 TB.

3.5 Discussion

3.5.1 Antenna

For antennas, we recommend based on current analysis of mass, cost, launch capacity, TRL and surface roughness, to consider antenna sizes 3-5m in diameter, with a strong inclination to not surpass a 3.5m diameter unfolding antenna. If the OASIS mission is selected in the upcoming MIDEX cycle, we recommend re-evaluating this recommendation. Achieving a highly efficient, lightweight model with a large aperture and high surface precision without compromising performance may be challenging. The baseline design, a Gregorian configuration, or axially displaced ellipse (ADE) optical design is a promising path. The unfurlable antenna manufactured by

Airbus is up to par in its aperture size (ranging from 2.5-5 meters), but would need further engineering development in its operating frequency, achieving a TRL of 4-6 is another promising path.

Other solutions like the 1) The monolithic antenna is of optimal size (2.5 meters) and weight. For this method to be successful in the future however, as demonstrated in the BLAST-TNG TRL 4-6, 2) Northrop Grumman AstroMesh unfurlable mesh antenna, spans a large spectrum of aperture size suitable for various applications. Its TRL is 4-6 due to its previous success rate during over 10 orbiting missions. It reaches the BHEX mission's required frequency, operating at frequencies of 100-300 GHz. 3) the inflatable antenna system is a hypothetical solution for the antenna, though the system is in early development. The system is conceptualized to operate at sub-par BHEX mission frequencies, from 6 to 60 GHz. Since it has only flown in an experimental mission aboard STS-77, the 77th flight of the Space Shuttle, whether it is qualified to perform in the relevant environment and orbit of the BHEX mission is unknown. Its TRL is a 3-4.4) We also assess the Microwave Limb Sounder (MLS) experiment, implemented in the NASA Aura spacecraft in 2004. While this system is capable of operating in target BHEX Mission frequencies, and even surpassed the stated maximum when used with heterodyne radiometers in several frequency bands, the diameter is only 1.6 meters. If the aperture size proves to be adequately sensitive for the relevant environments, the MLS system may be suitable for space VLBI. Future tests are necessary to mature its TRL of 4-6 within three years. All four solutions might not lead to a solution that could be mplemented within the relevant time scales.

3.5.2 Frequency Reference

The frequency reference both controls the synthesizer that generates the local oscillator frequencies in the receiver as well as provides a clock signal for the digital back-end. The frequency reference subsystem must meet three crucial engineering requirements. Firstly, the frequency reference must introduce a coherence loss of under 10% on a timescale of 10 seconds (due to atmospheric turbulence-induced phase noise fluctuations) at an observing frequency of 345 GHz. Secondly, to be compatible with the receiver and the digital back-end, the frequency reference shall output either a 10 MHz or 100 MHz signal. Lastly, the system must continuously measure the drift of the reference oscillator with respect to absolute time, with a precision of 1 ps/sec achieved when averaged over a period of 10 minutes, for the purpose of accurate data correlation.

Frequency reference options include the Active Hydrogen Maser, Ultra Stable Oscillator (USO), Deep Space Clock, Intermediate-Scale Optical Clock, Optical Frequency Division of a Cavity-Stabilized Laser, Optical Time Transfer, and the Microwave-based Time Transfer. For precision timing we recommend further development of the intermediate-scale optical clock with the USO as a back-up. This is due to the low TRL and high performance of intermediate-scale optical clocks contrasted with the high TRL and inconsistent performance of the USO. If such performance cannot satisfy the science team and mission requirements, we recommend adopting and developing a stand alone Space MASER system yet suggest that for such a selection a detailed budget is presented for the development.

3.5.3 Optical Communication Overview

For optical communication, we recommend to utilize the largest available ground stations, as well as adopting the TBIRD modems as a baseline and leverage the extensive existing heritage of that system. Power amplifiers and other components will be evaluated in real time as the mission configuration, and specifically its orbit, are established. We also find that expected development costs might be prohibitive for an explorers class mission; therefore, a full cost analysis will be required to support the selection of any specific solution to be established during the mission architecture phase of this study.

Optical laser communication is advantages due to fewer diffraction losses, greater bandwidth, and power flexibility. We projected LLCD, LCRD, TBIRD, Psyche, and Artemis II O2O missions onto BHEX requirements to gauge the most suitable timelines, cost, and TRL. we recommend establishing multiple ground stations at multiple locations. Four sites should provide sufficient availability for BHEX to operate optimally. The TBIRD Modem with ARQ, which can potentially be used for BHEX, is our closest potential technology, with a TRL of 6. The high-speed interfaces and 10 cm optical module are TRL 6. All ground terminal aspects here are TRL 8. However, the buffer is TRL 3, as none support the BHEX required data writing speeds. Space apertures could span from 5-15 cm, while ground could span 30-80 cm, with power levels between 1-10 W, for viable architecture solution that support the required data rates.

ACKNOWLEDGMENTS

Black Hole Explorer mission concept study was funded by the Internal Research and Development (IRAD) program at NASA Goddard Space Flight Center. Technical and concept studies for BHEX have also been supported by the Smithsonian Astrophysical Observatory and by the University of Arizona. We acknowledge financial support from the Brinson Foundation, the Gordon and Betty Moore Foundation (GBMF-10423), the National Science Foundation (AST-2307887, AST-1935980, and AST-2034306). This project/publication is funded in part by the Gordon and Betty Moore Foundation (Grant #8273.01). It was also made possible through the support of a grant from the John Templeton Foundation (Grant #62286). The opinions expressed in this publication are those of the author(s) and do not necessarily reflect the views of these Foundations. BHEX is funded in part by generous support from Mr. Michael Tuteur and Amy Tuteur, MD. BHEX is supported by initial funding from Fred Ehrsam.

The data that support the findings of this article are not publicly available due to privacy concerns. They can be requested from the author at eliad.peretz@nasa.gov.

REFERENCES

1. W. M. Kimmel, P. M. Beauchamp, M. A. Frerking, et al., "Technology Readiness Assessment Best Practices Guide," (2023).
2. "NASA Procedural Requirements, NPR 7123.1D," (2023).
3. "NASA Research and Technology Program and Project Management Requirements, NPR 7120.8A," (2018).
4. "Technology Readiness Assessment (TRA) Guide, GAO-20-48G," (2020).

5. S. Hirshorn, S. Jefferies, K. Vassigh, et al., "Final Report of the NASA Technology Readiness Assessment (TRA) Study Team," (2016).
6. "General Enrionmental Verification Standard (GEVS) for GSRC Flight Programs and Projects, GSFC-STD-7000A," (2013).
7. T. Sridharan, R. Lehmensiek, D. Marrone, et al., "The black hole explorer (bhex): Preliminary antenna design," Submitted to the SPIE Conference Series (2024).
8. N. Galitzki, P. Ade, F. Angilè, et al., "The next generation blast experiment," Journal of Astronomical Instrumentation **03** (2014).
9. G. Coppi, P. A. Ade, P. C. Ashton, et al., "In-flight performance of the BLAST-TNG telescope platform," (2020).
10. "Media lario." https://www.medialario.com/ (2023).
11. "Media lario completes the telescope assembly for the nasa jpl asthros mission." https://www.medialario.com/post/media-lario-completes-the-telescope-assembly-for-the-nasa-jpl-asthros-mission (2022).
12. "AstroMesh deployable reflector from Northrop Grumman will help nasa's jet propulsion laboratory map soil moisture globally." https://news.northropgrumman.com/news/releases/photo-release-astromesh-deployable-reflector-from-northrop-grumman-will-help-nasa-s-jet-propulsion-laboratory-map-soil-moisture-globally.
13. "Center of excellence mechanisms: Deployable mechanisms." https://www.airbus.com/sites/g/files/jlcbta136/files/2023-10/Airbus_Defence_and_Space_Mechanisms_Products_2023.pdf.
14. "L.Garde smart space technologies." http://www.lgarde.com/.
15. G. Bilyeu and R. E. Freeland, "In-step inflatable antenna experiment."
16. "Astromesh unfurlable mesh antenna." https://www.northropgrumman.com/wp-content/uploads/AstroMesh-DataSheet.pdf.
17. "Planck fact sheet." https://sci.esa.int/web/planck/-/47365-fact-sheet.
18. "WMAP frequency coverage." https://wmap.gsfc.nasa.gov/mission/observatory_freq.html.
19. "MLS instrument science." https://mls.jpl.nasa.gov/eos-aura-mls/instrument.
20. "The SWAS instrument – a more detailed description." https://lweb.cfa.harvard.edu/swas/swasinstdetails.html.
21. "Instrument: MWI (WSF-M)." https://space.oscar.wmo.int/instruments/view/mwi_wsf_m.
22. "(ACR) Airborne Cloud Radar / (CVR) CloudSat Validation Radar." https://airbornescience.jpl.nasa.gov/instruments/acr-cvr.
23. C. R. Harris, K. J. Millman, S. J. van der Walt, et al., "Array programming with NumPy," Nature **585**, 357–362 (2020).
24. J. D. Hunter, "Matplotlib: A 2d graphics environment," Computing in Science & Engineering **9**(3), 90–95 (2007).
25. H. Rana, K. Akiyama, E. R. Canavan, et al., "The black hole explorer (bhex) cryocooling instrument," Submitted to the SPIE Conference Series (2024).
26. H. Rana, "Advancing cryogenic systems for the next generation of astrophysics discoveries," IAF Technical Papers **74** (2023).

27. G. Morgante, D. Pearson, F. Melot, et al., "Cryogenic characterization of the Planck sorption cooler system flight model," Journal of Instrumentation **12016** (2009).
28. L. Duband, E. Ercolani, L. Guillemet, et al., "In-flight performance of the HERSCHEL sorption coolers - One year of operation," Cryocoolers **16** (2011).
29. The Event Horizon Telescope Collaboration, "First M87 Event Horizon Telescope Results. II. Array and Instrumentation," The Astrophysical Journal Letters , 875:L2 (2019).
30. "Radioastron." `http://www.asc.rssi.ru/radioastron/`.
31. N. Kardashev, V. Khartov, V. Abramov, et al., "RadioAstron-a telescope with a size of 300,000 km: Main parameters and first observational results," Astronomy Reports **57**, 153–194 (2013).
32. "Active on-board hydrogen maser for radioastron space mission vch-1010." https://www.vremya-ch.com/index.php/en/progects-en/spaceapplications-en/vch-1010-en-2/index.html (2024).
33. "PHARAO atomic clock agreement signed by ESA and CNES." `https://www.esa.int/Enabling_Support/Space_Engineering_Technology/PHARAO_atomic_clock_agreement_signed_by_ESA_and_CNES`.
34. "Accubeat ultra-stable-oscillator recent outstanding results." https://www.accubeat.com/uso (2022).
35. Certain equipment or instruments are identified in this paper in order to specify the experimental procedure adequately. Such identification is not intended to imply recommendation or endorsement of any product by NIST, nor is it intended to imply that the equipment identified are necessarily the best available for the purpose.
36. "JUICE." `https://www.esa.int/Science_Exploration/Space_Science/Juice`.
37. E. A. Burt, J. D. Prestage, R. L. Tjoelker, et al., "Demonstration of a trapped-ion atomic clock in space," Nature **595**, 43–47 (2021). Bandiera_abtest: a Cg_type: Nature Research Journals Number: 7865 Primary_atype: Research Publisher: Nature Publishing Group Subject_term: Astronomical instrumentation;Atomic and molecular physics;Quantum metrology Subject_term_id: astronomical-instrumentation;atomic-and-molecular-physics;quantum-metrology.
38. J. D. Roslund, A. Cingöz, W. D. Lunden, et al., "Optical clocks at sea," Nature **628**, 736–740 (2024). Publisher: Nature Publishing Group.
39. T. D. Schmidt, S. Schlüter, T. Schuldt, et al., "COMPASSO: In-orbit Verification of Optical Key Technologies for Future GNSS," 158–182 (2022). ISSN: 2333-2069.
40. "Vector atomic evergreen clock." https://vectoratomic.com/ (2024).
41. "Inflection tiqker clock." https://www.infleqtion.com/tiqker (2024).
42. A. D. Ludlow, M. M. Boyd, J. Ye, et al., "Optical atomic clocks," Reviews of Modern Physics **87**, 637–701 (2015). 00210.
43. B. A. C. O. N. B. Collaboration, K. Beloy, T. Bothwell, et al., "Frequency ratio measurements at 18-digit accuracy using an optical clock network," Nature **591**, 564–569 (2021). arXiv: 2005.14694.
44. B. Bachman, G. d. Vine, J. Dickson, et al., "Flight phasemeter on the Laser Ranging Interferometer on the GRACE Follow-On mission," Journal of Physics: Conference Series **840**, 012011 (2017). Publisher: IOP Publishing.
45. P. Amaro-Seoane, J. Andrews, M. Arca Sedda, et al., "Astrophysics with the Laser Interferometer Space Antenna," arXiv e-prints , arXiv:2203.06016 (2022).
46. M. L. Kelleher, C. A. McLemore, D. Lee, et al., "Compact, portable, thermal-noise-limited optical cavity with low acceleration sensitivity," Optics Express **31**, 11954–11965 (2023). Publisher: Optica Publishing Group.

47. I. Khader, H. Bergeron, L. C. Sinclair, et al., "Time synchronization over a free-space optical communication channel," Optica **5**, 1542–1548 (2018).
48. J.-D. Deschênes, L. C. Sinclair, F. R. Giorgetta, et al., "Synchronization of Distant Optical Clocks at the Femtosecond Level," Physical Review X **6**, 021016 (2016). 00010.
49. E. D. Caldwell, J.-D. Deschenes, J. Ellis, et al., "Quantum-limited optical time transfer for future geosynchronous links," Nature **618**, 721–726 (2023). Number: 7966 Publisher: Nature Publishing Group.
50. M. Fujieda, T. Gotoh, and J. Amagai, "Advanced two-way satellite frequency transfer by carrier-phase and carrier-frequency measurements," Journal of Physics: Conference Series **723**(1), 012036 (2016).
51. J. Olson, R. Fasano, A. Kortyna, et al., "Commercialization updates of a field-deployable compact optical atomic clock," in Institute of Navigation (ION) International Technical Meeting, (Long Beach, CA) (2024).
52. M. Ledbetter, J. Roslund, A. Cingoz, et al., "Integrated rackmount optical clocks," in Precise Time and Time Interval Meeting, (Long Beach, CA) (2024).
53. J. P. Wang, B. Bilyeu, D. Boroson, et al., "High-rate 256+ Gbit/s laser communications for enhanced high-resolution imaging using space-based very long baseline interferometry (VLBI)," in Free-Space Laser Communications XXXV, H. Hemmati and B. S. Robinson, Eds., **12413**, 1241308, International Society for Optics and Photonics, SPIE (2023).
54. C. M. Schieler, K. M. Riesing, B. C. Bilyeu, et al., "On-orbit demonstration of 200-gbps laser communication downlink from the tbird cubesat," (2023).